Measurement of hyperfine splitting and determination of hyperfine structure constant of cesium $8S_{1/2}$ state by using of ladder-type EIT

Jie WANG, Junmin WANG*, Huifeng LIU, Baodong YANG, and Jun HE
State Key Laboratory of Quantum Optics and Quantum Optics Devices of China (Shanxi University),
and Institute of Opto-Electronics, Shanxi University,
No. 92 Wu Cheng Road, Tai Yuan 030006, Shan Xi Province, P. R. China

ABSTRACT

The narrow electromagnetically-induced transparency (EIT) resonance peaks are observed with two low-power counter-propagating diode lasers in cesium (Cs) $6S_{1/2}$ - $6P_{1/2}$ - $8S_{1/2}$ ladder-type atomic system. To precisely determine the centers of resonance peaks, multiple background-free EIT signals are achieved using a novel scanning scheme in which the coupling laser driving Cs $6P_{1/2}$ - $8S_{1/2}$ transition is scanned and the probe laser driving Cs $6S_{1/2} - 6P_{1/2}$ is frequency locked. A temperature-stabilized fiber-pigtailed waveguide-type phase electro-optical modulator (EOM) and a stable confocal Fabry-Perot cavity are used as a precise frequency marker to measure the hyperfine splitting of Cs $8S_{1/2}$ state. The impact of the external magnetic field on the measurement is also investigated. Furthermore, the hyperfine structure constant (here it is the hyperfine magnetic dipole constant, $\boldsymbol{A}$) of Cs $8S_{1/2}$ state is determined to be $\boldsymbol{A}$ = 219.06 MHz ± 0.12 MHz based on the measured hyperfine splitting (Δ_{hfs} = 876.24 MHz ± 0.50 MHz).

Keywords: hyperfine splitting (HFS), hyperfine structure constant, ladder-type atomic system, electromagnetically-induced transparency (EIT), cesium atoms

1. INTRODUCTION

Precise measurement of hyperfine splitting (HFS) of atomic ground and excited states is necessary to explore the complete dynamics of the electron-nucleus interaction in the atom. The nucleus has a magnetic dipole moment, related to the spin angular momentum, and an electric quadrupole moment, related the spatial aspheric distribution of charges. The interactions of the nuclear magnetic dipole moment with the magnetic field created by the motional electrons, and the electric quadrupole moment with the gradient of the electric field at the nucleus location, give rise to hyperfine structure interaction [1]. New experimental approaches such as optical frequency combs (OFC) and narrow linewidth lasers together with laser cooling and trapping of atoms reach increased accuracy for high precision studies of hyperfine structure in atomic excited states [2-4]. This new wave of experiments has not only renewed the interest of theorists in predicting accurate electron-nucleus interactions, but also the atomic parity non-conservation (PNC) community. These calculations of hyperfine splitting in excited states, where electron correlations are less complicated, are more sensitive to nuclear structure details, such as nuclear deformation and its influence on the atomic wave function. The hyperfine splitting measurements present excellent benchmarks to test state-of-the-art ab initio calculations of the electronic and nuclear wave functions for future PNC measurements, though, to convert the experimental results into useful information about the parity-violating weak interaction, the data has to be compared to complex theoretical calculations [5].

The OFC has a perfect accuracy in frequency measurement, but it is too complicated and expensive to use widely. Fortunately, we usually concern about relative frequency or frequency interval between hyperfine components. This can be easily performed by nonlinear optical techniques such as acoustic-optical modulator (AOM), electric-optical modulator (EOM) and optical frequency analyzer as Fabry-Perot (F-P) cavity. In this paper, we obtain the high-resolution spectroscopy of hyperfine structure in atomic excited states using EIT without a Doppler background. The frequency interval calibration combines a temperature-controlled EOM and a stable F-P cavity, which allow us to reduce the complication caused by the calibrated frequency components. The systematic effect of Zeeman shifts is also investigated.

* *Corresponding author,* **Email: wwjjmm@sxu.edu.cn**

Photon Counting Applications IV; and Quantum Optics and Quantum Information Transfer and Processing, edited by Jaromír Fiurášek, Ivan Prochazka, Roman Sobolewski, Proc. of SPIE
Vol. 8773, 877311 · © 2013 SPIE · CCC code: 0277-786X/13/$18 · doi: 10.1117/12.2016842

2. EXPERIMENTAL SCHEMES

Fig. 1 shows the energy levels associated with the ladder-type EIT process. The center wavelength for $6S_{1/2} - 6P_{1/2}$ transition and $6P_{1/2} - 8S_{1/2}$ transition are 894.6 nm and 761.1 nm, respectively. The decay rate of intermediate state $6P_{1/2}$ is $\Gamma_2/2\pi$ = 4.57 MHz, and that of excited state $8S_{1/2}$ is $\Gamma_3/2\pi$ = 2.18 MHz. Typically, the EIT signal is observed by scanning the frequency of the probes laser, while locking the frequency of the coupling laser. Thus the signal-to-noise ratio (SNR) is still limited by the absorptive background. However, the EIT signal in our experimental scheme is background-free due to novel scanning scheme - the frequency of the probe laser is frequency locked to resonante with the Cs $6S_{1/2}$ (F=3 or 4) - $6P_{1/2}$ (F'=3 or 4) hyperfine transitions, while the coupling laser is scanned over the Cs $6P_{1/2}$ (F'=3 or 4) - $6S_{1/2}$ (F''=3 and 4) transitions. The background-free EIT signal exhibits the benefit for precise determination of the center frequency of the EIT resonance peaks.

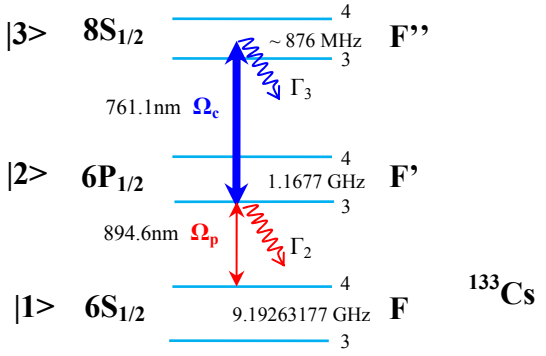

Fig. 1 Relevant hyperfine levels of ^{133}Cs atoms and the transitions involved in this work. The intense coupling laser with Rabi frequency Ωc drives |2> - |3> transition, while the weak probe laser with Rabi frequency Ωp drives |1> - |2> transition ($\Omega p < \Gamma_2$).

A schematic diagram of experimental setup is shown in Fig. 2 (a). A TO3-packaged distributed-feed-back (DFB) diode laser at 761.1 nm (Toptica) with typical linewidth of ~ 1 MHz serves as the coupling laser, which is scanned over the Cs $6P_{1/2}$ - $8S_{1/2}$ transition, while a TO8-packaged distributed-Bragg-reflector (DBR) diode laser at 894.6 nm (Photodigm) with typical linewidth of ~ 1 MHz is used as the probe laser. The latter one is frequency locked to the Cs $6S_{1/2}$ (F=4) - $6P_{1/2}$ (F=3) hyperfine transition by the conventional frequency modulation technique combined with saturattion absorption spectroscopy (SAS). In our experiment, the coupling and probe beams are in the counter-propagating (CTP) configuration to partly eliminate the Doppler effect when $\omega_p \sim \omega_c$. By contrast, we also investigate the co-propagating (CP) configuration. The CTP or CP configuration is selected by controlling the half-wave plate before PBS1. The two laser beams with a Gaussian radius ($1/e^2$ intensity) of 0.54 mm for the probe beam and 0.66 mm for the coupling beam overlapped in a Cs vapor cell (25 mm in diameter, 75 mm in length, is placed inside a three-layer permalloy μ metal tank for magnetic filed shielding with a residual magnetic field B < 0.2 mGauss) and then the probe beam was picked up by a board-band polarization beam splitter cube (PBS1) to the photodiode1 (PD1). The EIT spectra without a Doppler background from the PD1 are recorded by a digital storage oscilloscope (not shown in Fig. 2), and the frequency interval is calibrated by modulating the coupling laser using a fiber-pigtailed waveguide-type phase EOM (EOSpace) with a known radio frequency of 440.000 MHz and a confocal F-P cavity with a finesse of 120 and a free spectral range (FSR) of 2.5 GHz. The spectra including the carrier and the two first-order sidebands are recorded after the confocal F-P cavity by PD2 for calibrating frequency interval. The solenoid coil around the cell, which is placed inside the magnetic shielding tank, is used to exam the systematic effect arising from the longitudinal magnetic field. By comparison, we studied this effect when the two beams are circularly polarized by insert corresponding quarter-wave plates and two 45° dichroic mirrors, as in Fig. 2 (b). Considering the weak probe field for EIT, the power of probe beam is set at 1.14 μW (the intensity ~ 0.12 mW/cm^2). The power of coupling beam is set at 10.0 mW (the intensity ~ 730 mW/cm^2).

To reduce the systematic error from the calibrator combining EOM with a confocal F-P cavity, we take some appropriate measurements: 1) The DFB laser is chosen as coupling laser for better stability compared with ECDL, and its scanning is performed by modulating the current controller with triangle wave, rather than driving the piezo of ECDL's

grating extended cavity whose nonlinear effect is clearly observable; 2) The temperature of the large-bandwidth (~10 GHz) EOM is precisely controlled at 18.0 °C within ±0.005 °C; 3) The EOM is modulated at 440.000 MHz by using a rubidium clock stabilized signal generator (Agilent E8247D).

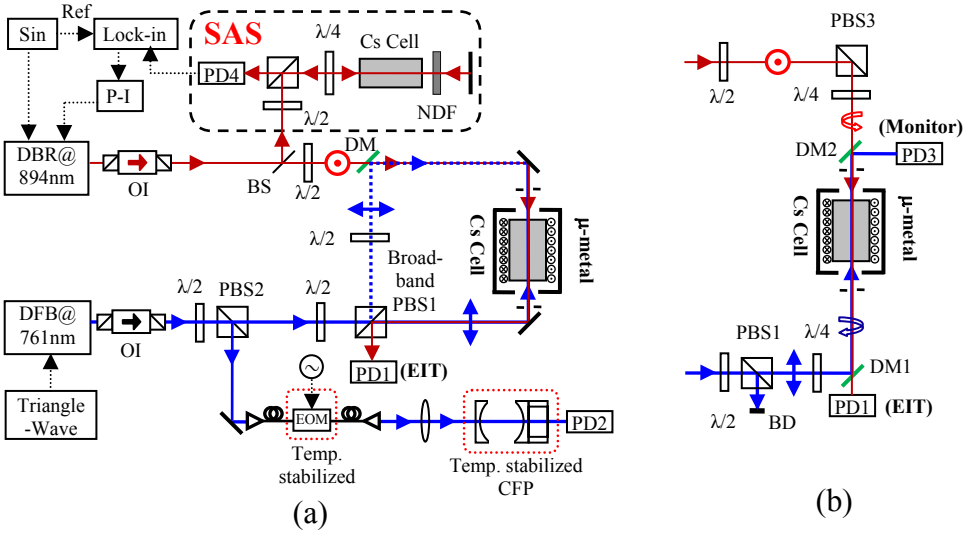

Fig. 2 Schematic diagram of experiment. The Cs vapor cell is placed inside a three-layer permalloy μ metal tank for magnetic filed screen (residual magnetic field B < 0.2 mGauss). (a) The two laser beams are linearly polarized and perpendicular each other ($(\sigma^+ + \sigma^-) - (\sigma^+ + \sigma^-)$) in front of the Cs cell; **(b)** The two laser beams are circularly polarized with the same polarization ($\sigma^+ - \sigma^+$ or $\sigma^- - \sigma^-$) in front of the Cs cell. Keys to figure: SIN: sine-wave signal generator; Ref: reference channel of lock-in amplifier; Lock-in: lock-in amplifier; PD: photodiode; SAS: saturated absorption spectroscopic device; P-I: proportion and integration amplifier; λ/2: half-wave plate; λ/4: quarter-wave plate; NDF: natural density filter; OI: optical isolator; PBS: polarization beam splitter cube; BS: beam splitter plate; EOM: fiber-pigtailed waveguide-type phase electro-optical modulator; CFP: confocal F-P cavity; DM: 45° dichroic mirror.

3. EXPERIMENTAL RESULTS AND SYSTEMATIC EFFECTS

In the ladder-type Cs $6S_{1/2}$ - $6P_{1/2}$ - $8S_{1/2}$ system (see Fig. 1), we note that two kinds of optical pumping effect, single-resonance optical pumping (SROP) and the double-resonance optical pumping (DROP), should be considered. The frequency of the probe laser is locked to the F=4 - F'=5 transition, and SROP will still transfer partial population on F=4 to F=3 level via F'=3 excitation and decay. Simultaneously, DROP will also transfer the partial population on F=4 to F=3 level via F=4 - F'=3 - (F''=3, 4) two-step excitation and (F''=3, 4) – (F'=3, 4) - F=3 and (F''=3, 4) - $7P_{1/2}$ (or $7P_{3/2}$) - F=3 decay channels. The SROP and DROP result in reduction of the population on F = 4 level, they will enhance the probe beam's transmission. So these SROP and DROP will be mixed with EIT, and it is a little bit difficult to distinguish them in experiments.

Fig.3 shows the comparison of probe signals of $6S_{1/2}$ (F=4) - $6P_{1/2}$ (F'=3) - $8S_{1/2}$ (F''=3) for CTP and CP configurations. For Fig. 3(a), the Rabi frequency of probe laser Ω_p of is 0.1 times less than the decay rate Γ_2, the SROP and DROP effects should be neglected. For a Doppler-broadened ladder-type atomic system, if the probe and coupling beams are arranged in the CP configuration inside the vapor cell, the atomic coherence will be mostly submerged by the Doppler effect, so the EIT signal is very difficult to observe unless the Rabi frequency of the coupling beam is bigger than the Doppler broadening ($\Omega_c > \Delta\omega_D$). This is why one needs a much intense coupling laser beam to observe the ladder-type EIT in the earlier experiments. If the probe and coupling lasers take the CTP configuration, the Doppler effect will be almost eliminated because the CTP configuration is two-photon Doppler-free in the ladder-type atomic system [6]. In this case, the ladder-type EIT only requires $\Omega_c > (\Delta\omega_D \times \Gamma_3)^{1/2}$, and is often much smaller than $\Delta\omega_D$, so Ω_c can be much smaller than $\Delta\omega_D$. Briefly, ladder-type EIT experiments in the CTP configuration do not need an intense coupling laser anymore [6], so we adopt the CTP configuration in our experiment in which two low-power diode lasers are utilized.

By contrast, we consider a little bit stronger probe beam, say $\Omega_p \sim \Gamma_2$, as shown Fig.3 (b). The SROP and DROP effects are notable. In CTP configuration, the EIT, SROP and DROP signals are mixed. In CP configuration, there is no contribution due to EIT under the condition $\Omega_c < \Delta\omega_D$, only the contribution of SROP and DROP.

By scanning the coupling laser's frequency, we record the EIT signal and the transmitted signal of the confocal F-P cavity from PD1 and PD2 by a digital storage oscilloscope, as in Fig. 4. The horizontal coordinates are calibrated by the 880.000 MHz frequency interval of the two modulation sidebands, which is close to the hyperfine splitting ~ 876 MHz for Cs $8S_{1/2}$ state and is fitted with multi-peak Lorenz function. The frequency interval of the two EIT peaks is determined by fitting them to theoretical formula of the ladder-type EIT in ref. [6]. The hyperfine splitting of Cs $8S_{1/2}$ state is labeled as $\Delta_{hfs} = \nu \pm \Delta\nu$, here $\Delta\nu$ refers to the fitting statistical error (within 95% confidence interval) which combines the F-P signal fitting statistical error with the EIT signal fitting statistical error. For 60 times measurements, the fitting errors $\Delta\nu$ range between 30 kHz and 60 kHz, mean 45 kHz. In the Cs $6S_{1/2}$ (F=4) - $6P_{1/2}$ (F'=3) - $8S_{1/2}$ (F''=3, 4) ladder-type hyperfine transition channel, we record 60 times and fit them to get the mean and standard error of mean, which gives (876.24 MHz ± 0.095 MHz), and 0.095 MHz respects systematic error.

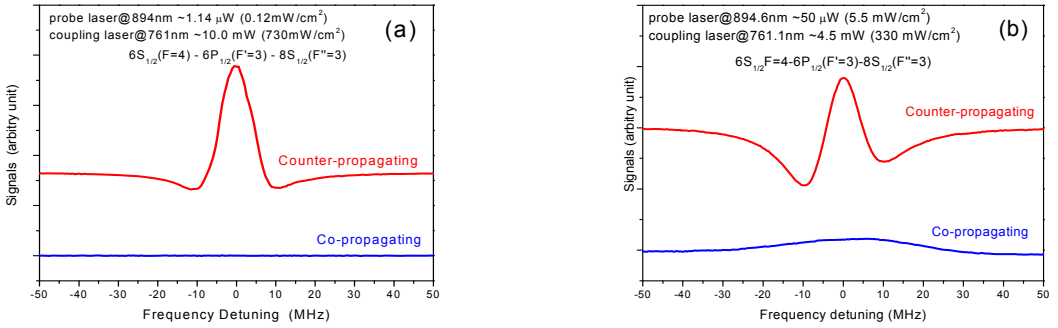

Fig. 3 Comparison of probe signals for $6S_{1/2}$ (F=4) - $6P_{1/2}$ (F'=3) - $8S_{1/2}$ (F''=3) in CTP and CP configurations. **(a)** The probe beam's intensity is 0.12 mW/cm^2 ($\Omega p < \Gamma_2$) and the coupling beam' intensity is 730 mW/cm^2. **(b)** The probe beam's intensity is 5.5 mW/cm^2 ($\Omega p > \Gamma_2$) and the coupling beam' intensity is 330 mW/cm^2.

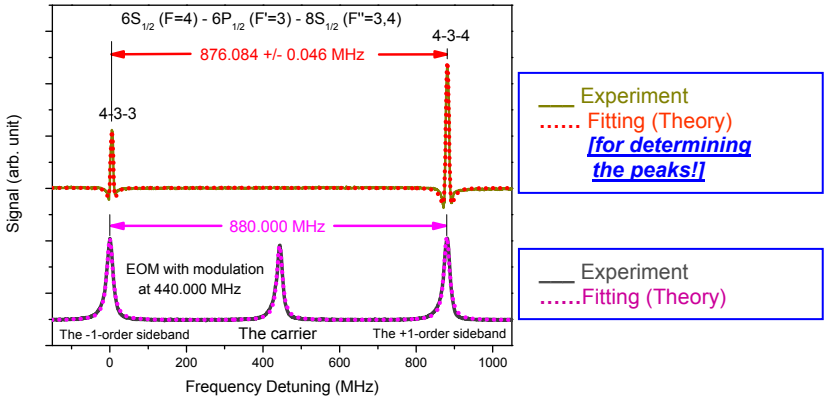

Fig. 4 Measurement of hyperfine splitting of Cs $8S_{1/2}$ state through hyperfine transition channel $6S_{1/2}$ (F=4) - $6P_{1/2}$ (F'=3) - $8S_{1/2}$ (F''=3, 4). The lower curve is transmission signal of the F-P cavity for the scanning coupling laser@761.1nm after the fiber-pigtailed waveguide-type phase modulator. The frequency interval between the +1-order sideband and the -1-order sideband are 880.000 MHz, which is determined by the EOM's driving RF frequency (stabilized by a rubidium clock). The upper curve is EIT signal. The Cs $6S_{1/2}$ (F=4) - $6P_{1/2}$ (F'=3) - $8S_{1/2}$ (F''=3) transitions are labeled as 4-3-3 and the Cs $6S_{1/2}$ (F=4) - $6P_{1/2}$ (F'=3) - $8S_{1/2}$ (F''=4) transitions are labeled as 4-3-4. The linewidth of EIT resonance peak is ~ 8 MHz. Both of the fitting curves show perfect agreement with experimental data. In this way the hyperfine splitting between F''=3 and F''=4 levels in Cs $8S_{1/2}$ state can be measured with a very small fitting statistical errors.

We also study the system effect of the external magnetic field on the measurement. For two-photon transitions between S states with $\Delta M_F = 0$, there is no linear Zeeman shift. Strictly speaking, when the laser beams propagate parallel to the magnetic field in Cs cell, π-transitions do not occur [1]. Each of the linearly-polarized laser beams in Fig. 2 (a) should be considered as the superposition of σ^+ and σ^- components with equal amplitudes. Although the power resonated on 6S – 6P transition is ~ 2% of the saturation, there exist some optical pumping that could couple with an external magnetic field. Due to the optical pumping between Zeeman sublevels, the populations of ground-state atoms are symmetrical distributed on Zeeman sublevels. Consequently, the magnetic field only broadens but not shifts the peaks by linear Zeeman shift. However, the laser polarization is not perfectly linear, thus the amplitude of two components are different, which lead to asymmetric effect. To investigate the effect of Zeeman shifts due to imperfect magnetic shield, the hyperfine splitting is measured in magnetic field generated by the solenoid coil as in Fig. 2 (a).

Fig. 5 shows the HFS vs. magnetic field. We find the slope to be 44(29) kHz/Gauss. In addition, we carefully investigate the dependence of HFS for different polarization combinations of probe and coupling laser on magnetic flux density. While the two lasers have the same circular polarizations as in Fig. 2 (b), we get a maximum slope of 970(27) kHz/Gauss (see Fig. 5). That is, the systematic uncertainty from the Zeeman shift for imperfect line polarization is ~ 2 orders of scales less than that for circular polarization. The reduced magnetic field along the axis of Cs vapor cell inside the magnetic shielding tank is measured to be less than 0.2 mGauss, which is ~ 10^{-3} less than geomagnetic field (~ 500 mGauss), we estimate the maximum possible uncertainty from the Zeeman shift is less than 0.03 kHz, which is negligible compared to the other uncertainties.

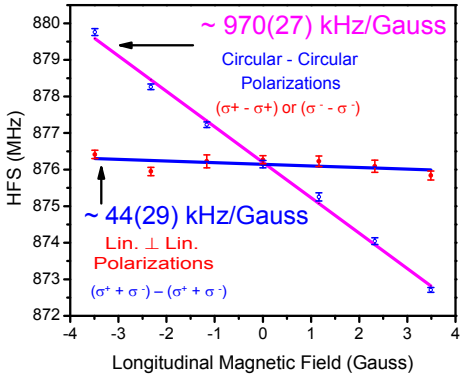

Fig. 5 When the longitudinal magnetic field inside the permalloy μ metal tank is applied by using a solenoid driven by a high-resistance constant-current DC power supply, the hyperfine splitting of Cs $8S_{1/2}$ state is measured with two different polarization configurations. The coupling laser beam (761nm) and the probe laser beam (894nm) are linearly polarized but are perpendicular each other (lin. ⊥ lin. configuration, corresponds to $(\sigma^+ + \sigma^-) - (\sigma^+ + \sigma^-)$, not π - π) in one case, and both laser beams are identically circularly polarized (circular-circular configuration, corresponds to $(\sigma^+ - \sigma^+)$ or $(\sigma^- - \sigma^-)$ in another case. Only statistical errors include in the error bar. The systematic uncertainty can be reduced by choosing linearly polarized lasers for insensitivity to magnetic field.

Besides Zeeman shifts, an accurate determination of the hyperfine structure splitting requires careful attention to a number of other possible systematic uncertainties such as: ac Stark shift, Zeeman shift, pressure shift, errors arising from misalignment of the CTP laser beams, the locking offset of probe laser, and uncertainty arising from the frequency interval calibration. The ac Stark shifts is measuered to be less than 492 kHz. To estimate the effect of pressure shifts, we monitor the temperature nearby the Cs cell to be ~23°C, corresponding to Cs vapor pressure of 1.2×10^{-6} Torr. Theoretically, the pressure shift is the same for the two hyperfine components F''=3 and F''=4 in Cs $8S_{1/2}$ state. But based on the previously measured shift of 6S-8S two-photon transitions, - 12(10) kHz/mTorr for F''=3 and - 26(10) kHz/mTorr for F''=4 in ref. [9], - 63.3 kHz/mTorr in ref. [10], we expect a shift of less than 0.1 kHz. The effect of misalignment of the two laser beams is to broaden and shift the peaks through a first-order Doppler shift. And the locking offset of probe laser can cause detuning to the resonance transition. But those two systemic shifts can be negligible since the relative intervals were used. Uncertainty of frequency interval calibration depends on the

nonlinearity of frequency scanning, the thermal fluctuation and mechanical vibration of F-P cavity, the uncertainty of radio frequency driving on EOM. A conservative estimate of the instability of frequency interval calibration is ~ 30 kHz mainly due to nonlinear scanning.

Combine the total systematic uncertainty of 493 kHz with the statistic uncertainty of 92 kHz, we obtain the total error of 501.5 kHz. Finally, the hyperfine splitting between F''=3 and F''=4 levels in Cs $8S_{1/2}$ state is determined to be Δ_{hfs} = 876.24 MHz ± 0.50 MHz. Therefore, the magnetic dipole constant for Cs $8S_{1/2}$ state is determined to be $\boldsymbol{A}$ = 219.06 MHz ± 0.12 MHz. The values agree to previous measurements: (218.9 MHz ± 1.6 MHz) [7], (219.3 MHz ± 0.2 MHz) [8], 219.12 MHz ± 0.01 MHz) [9], (219.125 MHz ± 0.004 MHz) [10] and (219.14 MHz ± 0.11 MHz) [11].

4. CONCLUSION

In conclusion, we have demonstrated a new technique for high-resolution hyperfine splitting measurement in atomic excited states by using of the ladder-type EIT. The experiments have been done using the Cs $6S_{1/2}$ - $6P_{1/2}$ - $8S_{1/2}$ ladder-type system with a Cs vapor cell around room temperature. The weak probe laser is locked to the lower transition while the strong coupling laser is scanned across the upper transition. The EIT peaks appear in the probe transmission whenever the coupling laser comes into resonance with a hyperfine level. In this arrangement the centers of EIT peaks are well determined by fitting the curves for they have no Doppler background compare to conventional EIT. The frequency axis of the coupling laser is calibrated by using a temperature-controlled EOM and a stable confocal F-P cavity to reduce the systematic errors. The EOM is modulated by a signal generator with a known frequency.

In this manner, we are able to measure hyperfine splitting of the Cs $8S_{1/2}$ state to be 876.24 MHz with a statistic error of 0.095 MHz. The systematic effect of Zeeman shifts is investigated. Combining the total systematic uncertainty of 493 kHz with the statistic uncertainty of 92 kHz, we obtain the total error of 501.5 kHz. Finally, the hyperfine splitting between F''=3 and F''=4 levels in Cs $8S_{1/2}$ state is determined to be Δ_{hfs} = (876.24 MHz ± 0.50 MHz). Therefore, the magnetic dipole constant for Cs $8S_{1/2}$ state is determined to be $\boldsymbol{A}$ = (219.06 MHz ± 0.12 MHz), which is consistent with previous measurements. This work provides a simple and universal method to measure excited-state hyperfine structure in other element atoms, which are of interest for PNC measurements.

ACKNOWLEDGMENT

This work is partially supported by the National Natural Science Foundation of China (Grant Nos. 61078051, 11274213, 61205215, 11104172, and 612279002), the Shanxi Scholarship Council of China (Grant No. 2012-015), the Research Program of Sci & Tech Star from Taiyuan, Shanxi Province, China (Grant No. 12024707), the Project for Excellent Research Team of the National Natural Science Foundation of China (Grant No. 61121064), and the National Major Scientific Research Program of China (Grant No. 2012CB921601).

REFERENCES

[1] C. J. Foot, Atomic Physics, Oxford University Press, New York, 97~105, 13~16 (2005)
[2] G. P. Barwood, P. Gill, and W. R. C. Rowley, "Frequency measurements on optically narrowed Rb-stabilized laser diodes at 780 nm and 795 nm," ***Appl. Phys. B*** 53, 142~147 (1991)
[3] A. Marian, M. C. Stowe, J. R. Lawall, D. Felinto, and J. Ye, "United time-frequency spectroscopy for dynamics and global structure," ***Science*** 306, 2063~2068 (2004)
[4] H. C. Chui, M. S. Ko, Y. W. Liu, J. T. Shy, J. L. Peng, and H. Ahn, "Absolute frequency measurement of rubidium 5S-7S two-photon transitions with a femtosecond laser comb," ***Opt. Lett.*** 30, 842~844 (2005)
[5] E. Gomez, S. Aubin, L. A. Orozco, and G. D. Sprouse, "Lifetime and hyperfine splitting measurements on the 7s and 6p levels in rubidium," ***J. Opt. Soc. Am. B*** 21, 2058~2067 (2004)
[6] J. Gea-Banacloche, Y. Q. Li, S. Z. Jin, and M. Xiao, "Electromagnetically induced transparency in ladder-type inhomogeneously-broadened media: theory and experiment," ***Phys. Rev. A.*** 51, 576~584 (1995)
[7] R. Gupta, W. Happer, L. K. Lam, and S. Svanberg, "Hyperfine-structure measurements of excited S states of the stable isotopes of Potassium, Rubidium, and Cesium by cascade radio-frequency spectroscopy," ***Phys. Rev. A*** 8, 2792~2810 (1973)

[8] P. P. Herrmann, J. Hoffnagle, A. Pedroni, N. Schlumpf, and A. Weis, "Doppler-free spectroscopy of the 8S state of Cs," ***Opt. Commun.*** 56, 22~24 (1985)
[9] G. Hagel, C. Nesi, L. Jozefowski, C. Schwob, F. Nez, and F. Biraben, "Accurate measurement of the frequency of the 6S-8S two-photon transitions in cesium," ***Opt. Commun.*** 160, 1~4 (1999)
[10] P. Fendel, S. D. Bergeson, Th. Udem, and T. W. Hänsch, "Two-photon frequency comb spectroscopy of the 6S-8S transition in cesium," ***Opt. Lett.*** 32, 701~703 (2007)
[11] J. E. Stalnaker, V. Mbele, V. Gerginov, T. M. Fortier, S. A. Diddams, L. Hollberg, and C. E. Tanner, "Femtosecond frequency comb measurement of absolute frequencies and hyperfine coupling constants in cesium vapor," ***Phys. Rev. A*** 81, 043840-1~043840-12 (2010)